UCONN
LIBRARY

Holster Scholar Projects

Honors Scholar Program

Fall 2021

Assessing the Feasibility of a Belt Based Continuously Varied Transmission for Bicycles

Ethan Wicko
University of Connecticut - Storrs, ethan.wicko@uconn.edu

Assessing the Feasibility of a Belt Based Continuously Varied

Transmission for Bicycles

Ethan Wicko

Mentor: Dr. David M. Pierce

Abstract

The objective of this project is to establish the feasibility of a new drivetrain that decreases maintenance and decreases rider effort compared to current widely used derailleur-based drivetrains by utilizing a belt based continuously varied transmission. With further development, this technology will make cycling more accessible by reducing the mechanical knowledge required to maintain a functional bike and facilitate bicycle riding by increasing durability and providing infinite gear ratios within that range, potentially increasing the health and quality of life for many.

Introduction

Transmissions are a fundamental part of modern bicycles, enabling riders to minimize the amount of effort they expend while riding a bike by keeping their pedaling cadence within the range that the rider is most efficient. This optimal pedal cadence (around 80 rpm for most riders) allows the rider to improve their power expenditure per unit time (minimizes muscle activation per unit time). The effect of deviating from an optimal pedal cadence is significant, as seen by a 5-6% increase in energy cost by changing the cadence 20 rpm (from 80rpm to 100rpm) (Stebbins, Moore, and Casazza, 2014). This shows the significance of using a drivetrain that can change the mechanical advantage (gear ratio) and thus aim to keep rider cadence as close to optimal as possible while the rider crosses terrain with varying grades (steepness) and ground consistency/hardness.

Since conventional derailleur-based drivetrains, seen in Figure 1, are completely exposed, they are vulnerable to environmental contaminants and impacts with objects that lead to frequent maintenance or part replacements. Additionally, rider effort is often wasted due to rider pedal cadences not matching the rider's optimal cadence. New technology in belt drives has resulted in a cogged belt drive that is equally efficient to a chain drive used in a DBD at 200 Watts (transmitting ~98% of the input power) (Denham, 2019a). Additionally, cogged belt drives are lighter than chains, always silent, and require virtually no maintenance as they are impervious to their environment. Cogged belt drives require no lubrication, alleviating a chain's inevitable loss of lubrication over time and tendency for small debris to stick to itself. Coupling a belt drive with an enclosed transmission creates a drivetrain that is virtually impervious to the outside world.

Figure 1, Derailleur based drivetrain

The goal of this project is to assess the feasibility of a continuously varied, belt-based transmission for use in bicycles. A belt based continuously varied transmission (CVT) works off of the principle that you can change the effective belt radius while the transmission is spinning by changing the distance between the cone shaped halves of two pulleys. The distance changed between two halves on one shaft would force the belt out concentrically around that shaft. By changing the effective radius of the belt as it is pulled around the pulleys, it is possible to change the mechanical advantage of the system in a similar way as that of when you change gears on a bike, where speed and torque are swapped (in different ways depending on how the system is set up). If the distance between the shafts is fixed, then the other pulley needs to adjust in a inverse direction of the same magnitude. This is because the circumference of the belt cannot change and the increase in effective radius of the belt at one pulley equates to a larger effective

circumference of the belt around the pulley, thus taking up more of the belt's total circumference. This method of adjusting mechanical advantage has been used in snowmobile transmissions for over 30 years and has been recently emerging in production cars with brands such as Nissan and Subaru implicating belt based CVT's more often. A diagram of a CVT used for car can be seen in Figure 2.
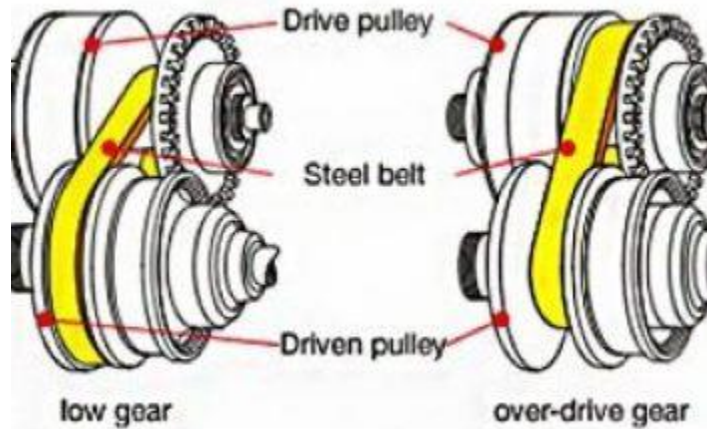
Figure 2, Diagram of Automotive CVT

Traditionally, the fields that CVT's have been used in allow for some amount of slippage, operate at high rpms, transmit a large amount of mechanical power, are able to use high rpm methods to actuate the pulley sheaves (with ways such as cams activated by centripetal forces of large magnitudes), are able to take up a lot of space (relative to the space available on a bike), and are able to weigh a lot. All of these situations are not possible on a bike, thus it is very important to test whether or not the fundamentals of a redesigned belt based CVT will work for the environment that bikes provide.

The feasibility testing will be achieved by building a prototype with pulley halves that are small enough to fit between the feet of a cyclist then testing the following fundamentals: efficiency in different configurations, friction between the pulleys and the belt, as well as relative strength. The prototype will be built using a readily available neoprene belt. While not built specifically for low torque low rpm, the cost of creating a custom belt is far too great to make using one on prototypes or even the first final design practical due to the extremely low volume of belts that would be used for the prototyping process.

If possible, the implication of this transmission into a bicycle drivetrain (coupled with an extremely reliable, low maintenance, and efficient belt drive system) would be able to provide more accessibility to cycling by decreasing the amount of maintenance required to regularly ride a bike, as well as lower the amount of effort expended while riding. This increased accessibility to cycling could potentially have a sizable effect on the physical and psychological health of many.

Materials and Methods

To test the fundamentals of this drivetrain, a series of tests were conducted, however before any could be conducted, a working prototype had to be designed and assembled. The design for the prototype took place using a CAD software called Solidworks, and the prototype

would mainly consist of two cone shaped fixed pulley halves and two cone shaped sliding/actuatable pulley halves. The pulleys had a bore and the angle of the slope of these cones was determined to be 11 degrees. One of each type of pulley half would be paired together to create two full pulleys of which the distance between the halves could be adjusted. Two iterations of the pulley halves were designed and created, with fairly significant design differences between the two. In the first iteration of the pulley half, a key was attached to the pulley halve bore (extruded from the bore and made of the same Nylon material as the pulley) and no thickness outside of the thickness created by the slope of the cone. The second iteration was thicker and had a keyway in the bore. Also, the radius of the second iteration pulley was about 50% larger than the size of the first iteration pulley.

The CAD drawings were 3D printed using a proprietary firmament Onyx from the company Markforged. This filament is a composite composed mainly of nylon filled with micro carbon fiber that can achieve strengths greater than that of other common filaments such as plain nylon or ABS plastic (Markforged, n.d.). One first iteration fixed pulley half was printed using this filament and the second iteration was printed (in both the fixed and actuatable configurations) and machined from series 7000 MIC6 Cast Aluminum disks. A brass bushing was also designed and fabricated using 360 Brass, on which a pulley would be attached to. It

Figure 3, Close-up of actuation method

would be aimed at allowing the pulley to slide along the shaft. The halves of the pulleys were then attached to a keyed shaft and (except for the first pulley iteration) a key was placed in the broached keyways in both the bore of the pulley and on the shaft. The shafts were then attached to pillow block bearings that were attached to a supporting mount. The actuation method of the prototype was created by attaching a shaft collar to retain a spring on one end that would push on the actuatable pulley half. This would enact a preload on the pulley half which would transfer the force to the belt. Due to the sloped nature of the pulley halves, the belt will be forced outward concentrically about the pulley until the tension force acting on the belt and the outward component of force created by the spring preload are equal. The preload of the spring would be controlled by removing force acting on the pulley by applying an opposing force via manually pulling on a thrust bearing on the side of the spring touching the pulley. The thrust bearing would be able to rotate in the opposite direction of the shaft motion, allowing the application point of the manual force to not rotate around the shaft, as shown in Figure 3. This was tested by setting up the thrust bearing and springs and manually pulling on the washer of one spring thus decreasing the preload applied to one of the sheaves. The motor was then run, giving the forces acting on the belt an opportunity to reach equilibrium as the belt was circulated.

The first of these included testing the efficiency of the drivetrain. Equipment for testing the efficiency was designed, using a motor to supply mechanical power to the transmission prototype and a load was applied using a magnetic resistance device commonly found on exercise bicycles. A motor rated for 250 Watts (W) was used and bolted directly to a large sheet of (¾") plywood that would act as a base for the drives that would transfer power into and out of the transmission. The motor was then connected to a shaft that changed the mechanical advantage of the motor. The shaft was suspended by bearings fitted into a laser cut plywood support base that was directly screwed into the large plywood base. This shaft that changed the

Figure 4, First half of prototype shown on left, second on right

mechanical advantage was then connected to the transmission prototype via another chain drive. The halves of the prototype can be seen up close in Figure 4 and the first half of the prototype was screwed directly to the plywood base. The second half of the prototype was then attached to a smaller piece of plywood that would be able to be moved and clamped down in various locations as a way to change the distance between the two halves of the prototype and change the belt tension when the pulleys would have a fixed distance between each other. The second half of the prototype was then attached to a bike wheel via a chain drive. The bike wheel was directly touching the roller on the magnetic resistance device, both of which were mounted onto the same smaller piece of ¾" plywood. This setup enabled the chain drive connecting the second half of the prototype to the bike wheel to maintain a constant tension by moving and clamping down the bike wheel in tandem with the second half of the prototype where needed. Figure 5 shows the full assembly of the testing equipment.
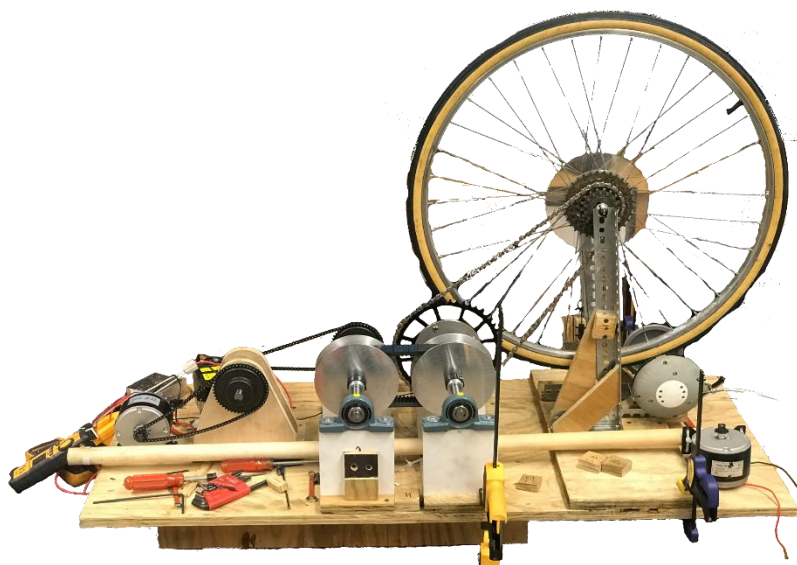
Figure 5, Full assembly of testing equipment

To test the efficiency, first, a control test was run. Efficiency for a mechanical system is fundamentally a comparison of the mechanical power (in watts) supplied to the system to the watts with the mechanical power the system is able to output. Access to an accurate power meter was not possible, so the output mechanical power was not able to be calculated. Since the supplied electrical power to the system could be measured, the difference in supplied power when the belt is in the system to that when the belt was not in the system would show how much less than 100% (or baseline/control) efficiency the belt made the system, thus showing the efficiency of the belt.

To supply electrical power to the motor, two 12V 9Ah batteries were connected in series to produce a maximum DC voltage of 24V supplied to the motor. The power supplied to the transmission was varied by changing the current and voltage supplied to the motor. A pulse width motor controller (pwm motor controller) was used to vary the effective voltage supplied to the motor, and the current was proportional to load applied to the motor, varied by the resistance setting on the magnetic resistance device or the wheel speed (until the maximum current that the system could support). A current overload fuse was also used to ensure that the applied current did not exceed a predetermined cutoff current of 25A. Motor Burnout would occur at a higher rate when the current is above the 14A rating for the motor, thus for all efficiency tests, the current was kept at about half of the rated current. To test the friction between the belt and the pulley, the motor was briefly overdriven to provide the most power the system could support.

For each test, the motor was used to spin the wheel to a speed of 20km/h. Because the resistance supplied by the magnetic resistance device is constant at a given speed and resistance setting, this would ensure that the load on the transmission prototype would remain the same throughout the belted and control tests. The magnitude of this resistance is not necessary in calculating the resistance since efficiency is relative and a ratio, as long as it remains the same. Wheel speed was measured using a bicycle cyclometer/ speedometer and was accurate to a tenth of a km/h, sufficient enough for this experiment.

For the first part of the efficiency ratio, the main prototype assemblies would remain on the plywood base, and a chain drive would run from the shaft that changed the mechanical advantage to the second half of the prototype, while running over a cog of equal number of teeth on the first half of the prototype. The shaft on the second half of the prototype would then be connected to the bike wheel as described above. Since all of the bearings and moving parts were engaged with or without the belt, the only difference between the control test and the subsequent belt tests would be the length of one chain drive growing by about 50% (the effect of which would be negligible) and the addition of the belt. The control power was measured by spinning the wheel to a speed of 20km/h at the magnetic resistance device's lowest resistance level and recording the voltage and current supplied to the motor (the power in).

The second part of the efficiency ratio was calculated by reverting the setup of the efficiency testing device to that described above. Many belt tests were performed using two different belt configurations, different radii configurations, and different tension configurations

for each radius. The distance between all of the pulley halves was set at the beginning of each belt test to set a constant effective belt radius. The same distance was used for both pulleys on the first half of the prototype and the second half, making sure that the transmission did not alter the mechanical advantage of the system and thus the load put on the motor (which would create completely inaccurate efficiency results). Distance between pulley halves and effective belt radius (of outer belt surface) was measured using calipers. The tension of the belt was then set by sliding the second half of the prototype farther away from the first half and clamping it to the plywood base. The placement of the bike wheel assembly was also adjusted to keep the tension in the chain drive between the second half of the prototype and the wheel constant between the tests. After spinning the transmission to help the tension in the belt equalize among all parts, the tension in the belt was measured by applying a force to a lever arm as seen in Figure 5. The center of the lever arm was attached to the center of the belt in the current configuration using a zip tie. The length of this lever arm and the weight applied to it need not be measured since it was constant among all of the tension measurements, thus the force applied to the belt to cause a displacement perpendicular to the belt length would be constant across all configurations. This displacement was then divided by the length of the belt from the center of the shaft to the center of the opposite shaft in order to obtain a tension ratio that would be used as a metric to compare the tension between different configurations used when testing efficiency. Power was increasingly supplied to the motor until the bike wheel was spinning at a speed of 20km/h on the lowest resistance setting of the magnetic resistance device. The current and voltage supplied to the motor to run at this specific load was measured.

The process of measuring the electrical power required at the given resistance level created by the magnetic resistance device was repeated many times for each of many configurations. These included a wide belt (with a width of 1.1875in) at varying effective belt radii of 1.511in, 2.107in, and 2.304in and a narrow belt (with a width of 0.88in) at effective belt radii of 1.088in, 1.816in, and 2.494in. Three tension levels were recorded for each effective radius. Again, the effective belt radius was varied by varying the distance between the pulley halves. Thus, for each iteration of a belted test described above, by taking the ratio of the control wattage (power imputed without the addition of the belt) to the test wattage (power imputed with the at the same resistance level (measured by wheel speed) the relative efficiency of the system due to the addition of the belt was calculated,

To test the friction between the pulley and the belt, the motor was over-driven (more current was supplied than what it was rated for) to a maximum of 438.44W. At this wattage, using an equation for calculating motor torque (Ozdemir, et al. 13, 2014), a torque of 57.9 Nm was produced on the drive shaft of the transmission. The tension was within the relative range used in the efficiency tests the efficiency of the motor was estimated to be 90%.

Strength of the prototype was assessed during the efficiency testing, not using metrics, but rather relative and observational preliminary strength assessments. The strength of key prototype components was assessed using the Finite element analysis capability of Solidworks simulation software. Finite element analysis is a method used by computers for analyzing the

effect of simulated real-world forces on a computer modeled object. Using an estimate that a professional cyclist can apply up to about 180 nm of torque to the crank arm of a bike (Rouffet, 2021) a simulation was run to assess the stress imposed upon key parts by the torque that would be exerted on the shaft due to intense pedaling.

       A bolted connection to the actuation device was assessed. This connection would be used on future prototypes regardless of the specifics of the device. To conduct the test, the material properties were set to steel (eFunda, n.d.) for the shaft and key (data was supplemented with the Solidworks materials database), brass for the bushing (Rudd, 2013) (properties supplemented from the Solidworks materials database), and 7075-T6 aluminum (found from the Solidworks materials database). The separate parts were modeled in a Solidworks assembly and contacts were set between the parts so that they would behave like solid bodies where they interfaced. A bearing fixture was applied to the bushing and pulley half in order to ensure that the torque did not produce a linear force. The Pulley half was also connected to the bushing using a preset bolt function of Solidworks modeled after a 4-40 screw with a preload set to 3Nm. One end of the shaft was fixed while a torque of 90Nm was applied to the pulley half, thus the torque could be transmitted through all of the interfaces. The stress imposed by the applied torque was recorded during a static simulation. this static simulation was then used in a fatigue simulation in order to calculate the life of the part by applying the torque in a cyclical manner and measuring how many cycles the part can withstand before suffering a fatigue failure.

       To better understand how much geometry of key components affects the strength and life of the components, three shafts of the same metal and arbitrary mass (same amount of material used) but different geometries were tested. The geometries of these configurations included a solid splined shaft, a hollow splined shaft, and a solid keyed shaft. The length and amount of material/ mass stayed the same as shown by the volume of the shafts being 23871 ±11 cubic millimeters (mm^3). The volume was 23885.3 mm^3 for the solid splined shaft, 23888.62 mm^3 for hollow splined shaft, and 23866.04 mm^3 for the solid keyed shaft.

       For all shafts, the material properties were set to be those of carbon steel (eFunda, n.d.) and the Solidworks materials database. One end of the shaft was fixed while the other end had a torque of 180Nm applied to it. The stress imposed by the applied torque was recorded for each of the configurations during a static simulation. these static simulations were then used in fatigue simulations to calculate the life of each configuration. For all of the fatigue simulations described above, 0-based loading was used for the simulations. This meant that the torque was applied maximally then the part returned to 0 load to consist of one cycle.

Results

When the preload was reduced, it was observed that friction between the shaft and the bore of the second iteration aluminum pulley half was too great and that it caused the pulley to not be able to move linearly along the shaft. The second iteration composite nylon actuating pulley half (pulley fitted onto brass bushing) was also observed on the prototype shaft to have the same buckling effect when a one-sided force was applied. Thus, it was found that the actuation method proposed in the first prototype would not work. This meant that, for the efficiency testing, the tension of the belt could not be set using a preload on the pulley half as originally designed, but meant that the tension would need to be figured out, not as an exact metric as a result of a known preload force, but as a relative metric as described in the materials and methods section.

Figures 6 and 7 show the results of the efficiency test. Different belt tensions defined by the belt tension ratio (the measure of displacement due to a given force over belt section length) produce varying efficiencies and are plotted below. The lines indicated on the figures general trendlines for the data points plotted.
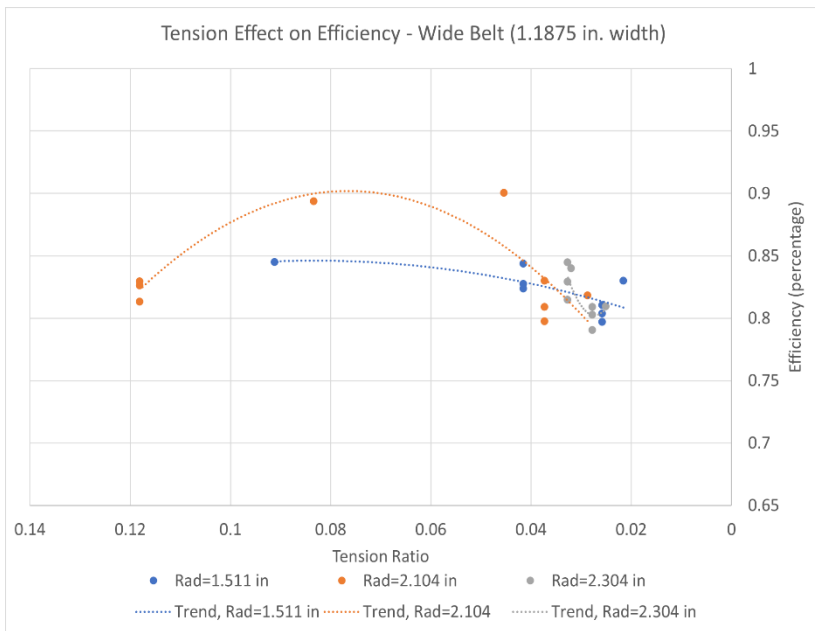
Figure 6
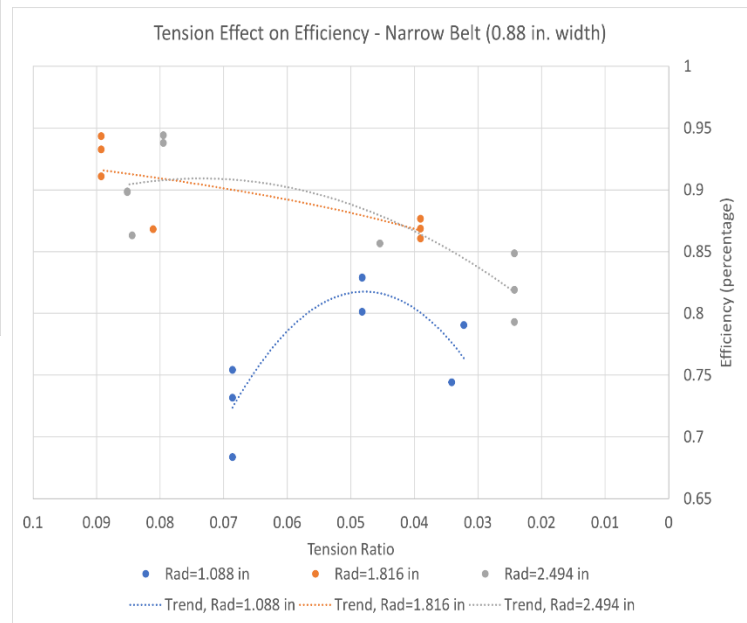
Figure 7

The following figures (8 and 9) further define the results of the efficiency test by more clearly comparing the occurrence of various efficiencies but separated by the change in belt width (which affects the belt cross sectional area without affecting the contact patch size).
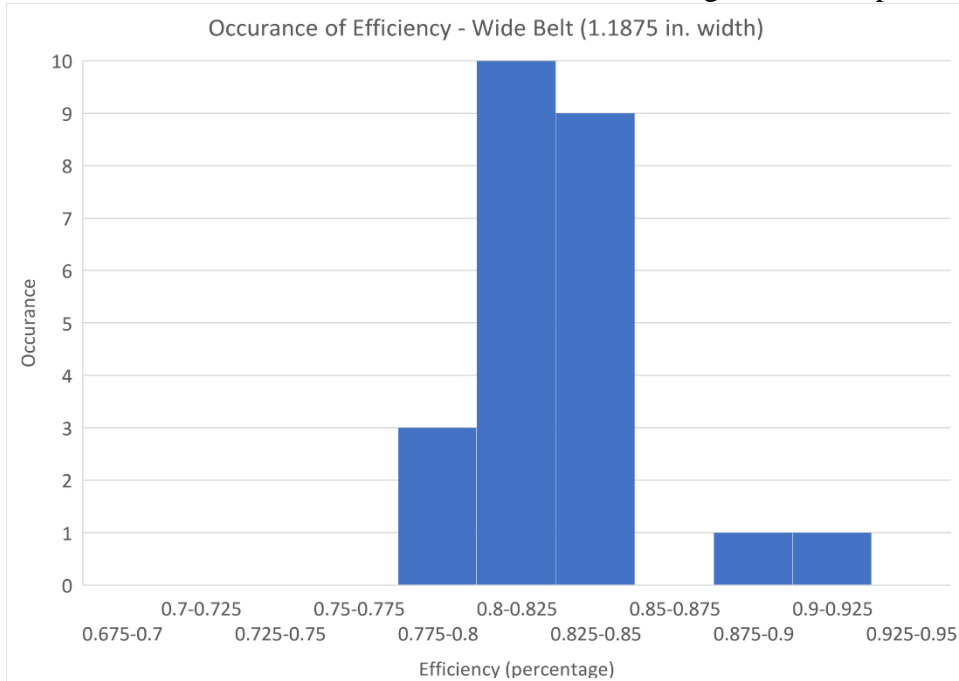
Figure 8
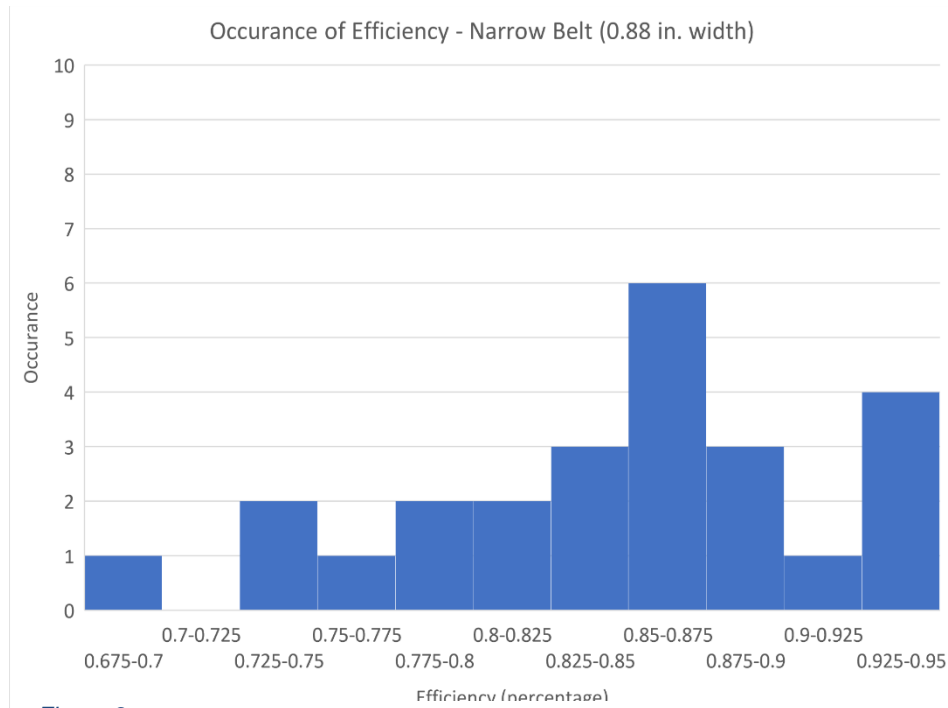
Figure 9

The following histograms (figures 10 and 11) break down the occurrences of efficiency by not only belt width but also by relative radius size (small medium and large). Using these histograms, other patterns can be seen, specifically regarding the ties between radius, tension, and efficiency.
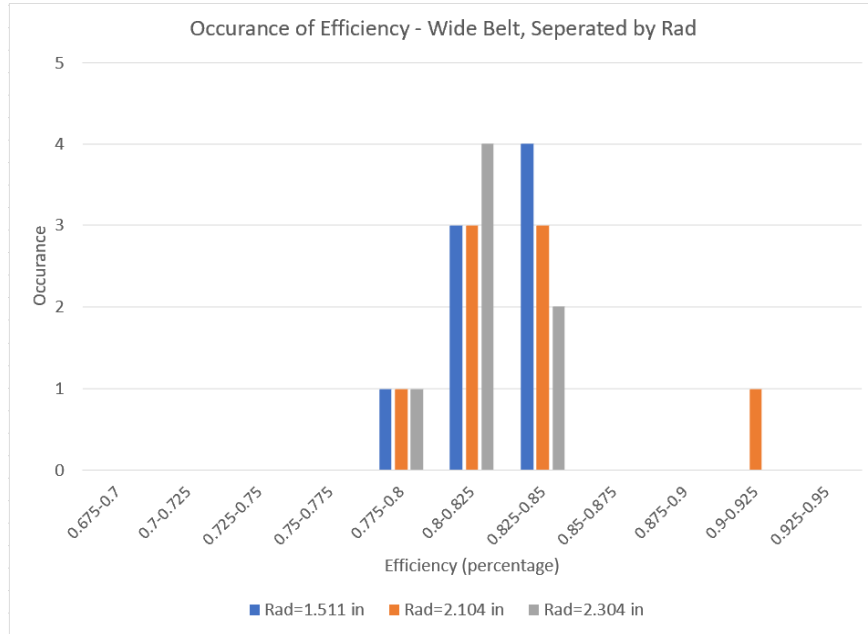
Figure 8
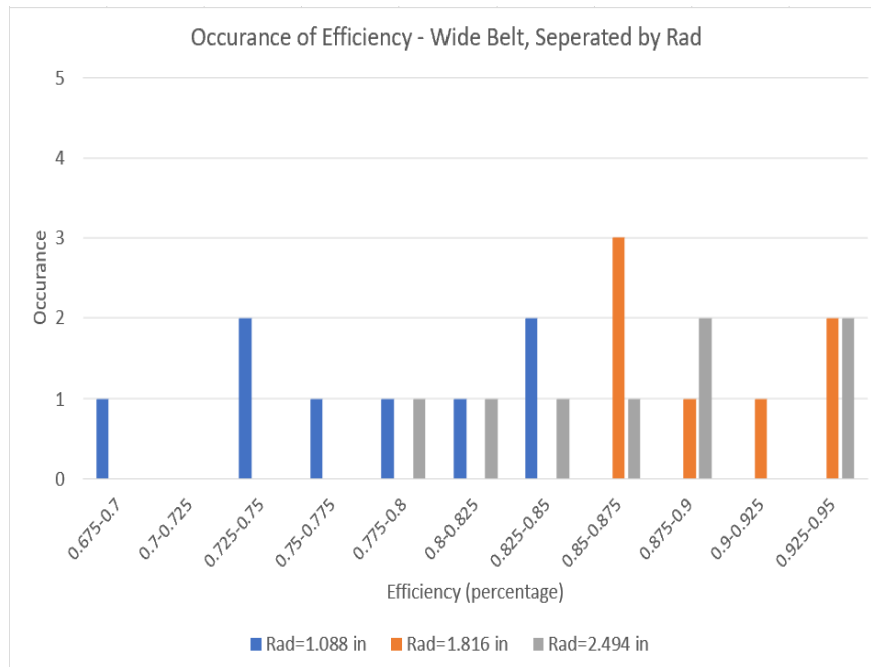
Figure 9

With the efficiency testing, we see that a decrease in efficiency means that there was a greater load on the motor with the addition of a belt. This load was caused by an increase in the friction of the system (thus resistance in addition to the resistance created by the magnetic resistance device).

The findings from the observational preliminary strength assessments were different based on the iteration of the pulley halves and the material used. The only part of the prototype that experienced visible structural failure was the first iteration of the fixed pulley. Made out of composite nylon with an extruded composite nylon key, it was found that when the motor was overdriven to test the slippage potential, the extruded key was partially ripped from the surface of the bore and forced into the surface of the bore. The exact torque exerted on the shaft that caused this failure is unknown as the part broke during a preliminary test, however it does expose the failure of this design nonetheless. The strength of the second iteration pulleys as well as the prototype as a whole seemed to be adequate, with most of the parts seemingly over-built. None of the other parts saw any visible signs of structural failure.

Figure 12 shows the stresses imposed by the torque on the method of attachment of the pulley to an actuation device. This actuation device was the bushing that was fabricated and briefly tested to see if sliding was possible, however the attachment to other actuation methods of a pulley half (such as a linear bearing or another type of bushing) would be connected in the same fashion. Figure 13 shows the life of the part.
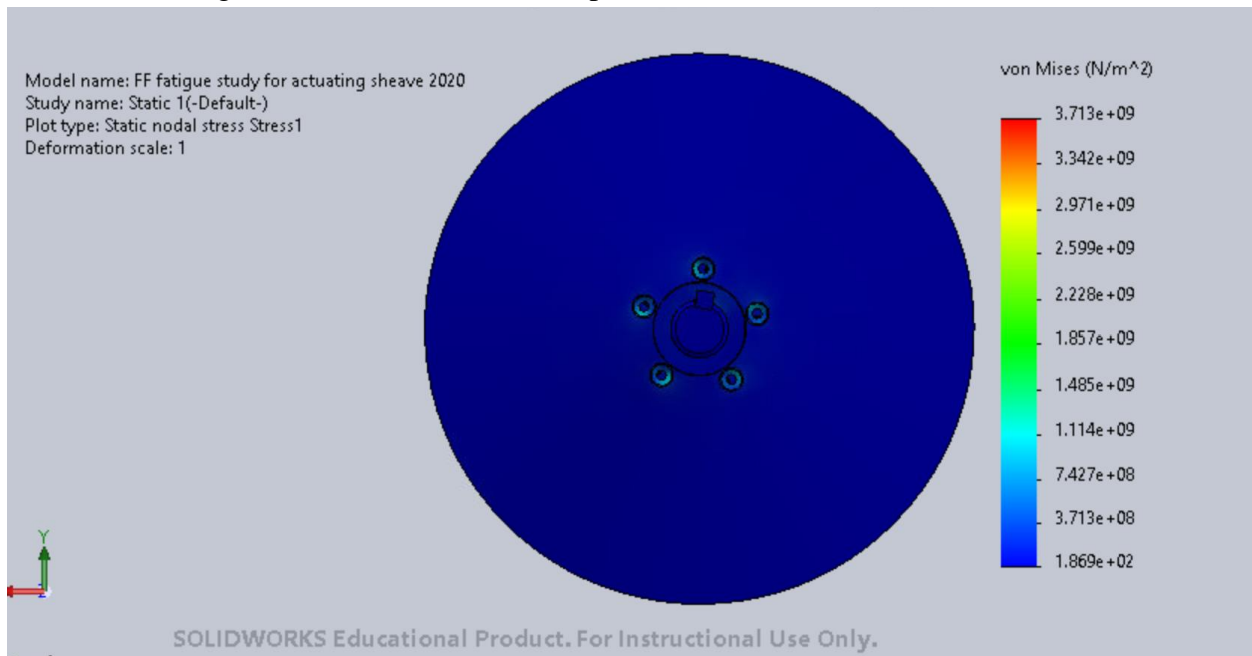
Figure 10
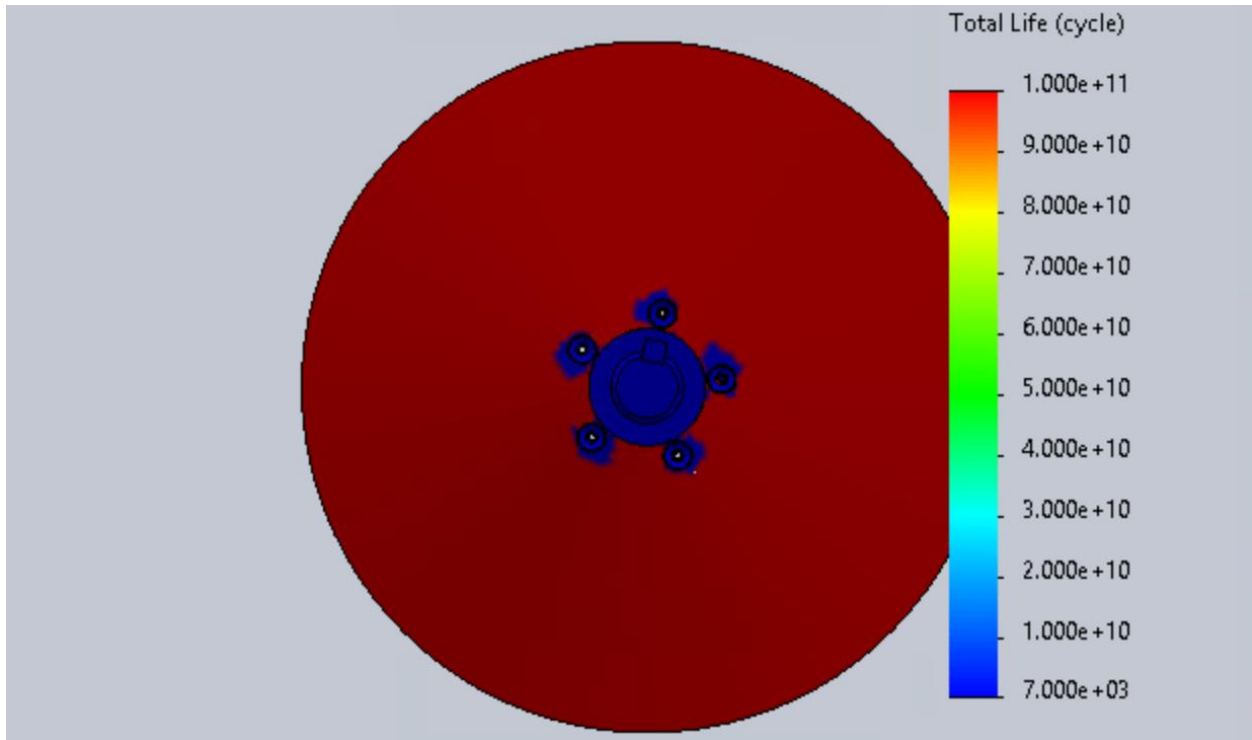
Figure 11

In the following figures (14-19) the stresses imposed by the torque and the life of the shaft configurations are shown. The configurations include figures 14-15 for the solid splined shaft, 16-17 for the hollow splined shaft, and 18-19 for the solid keyed shaft.
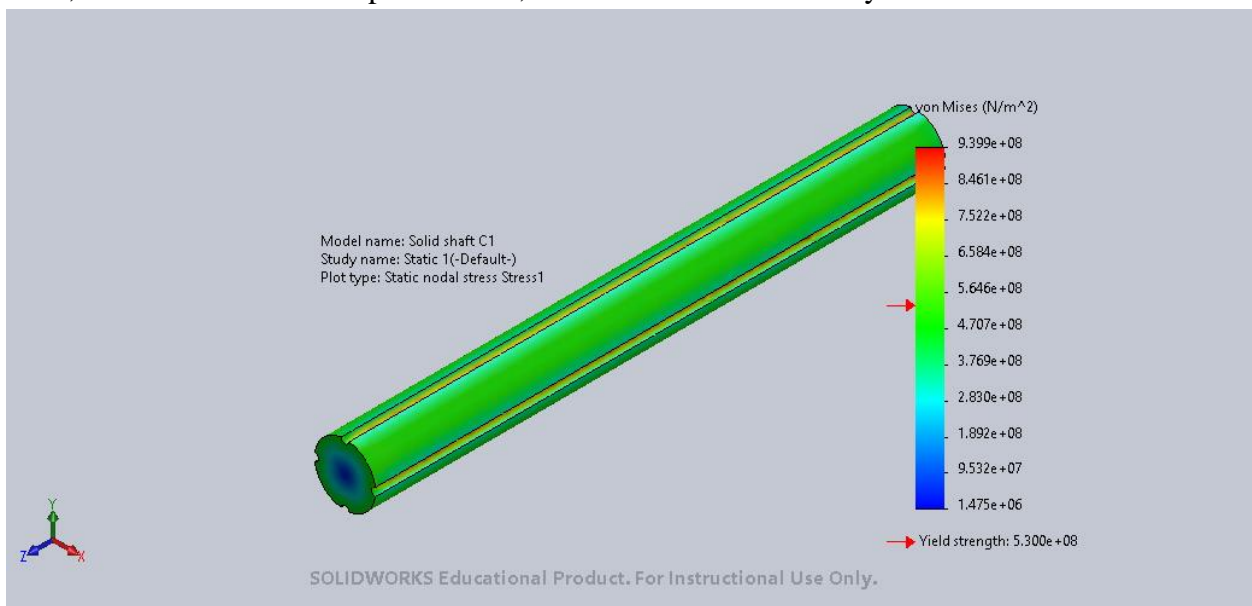
Figure 12
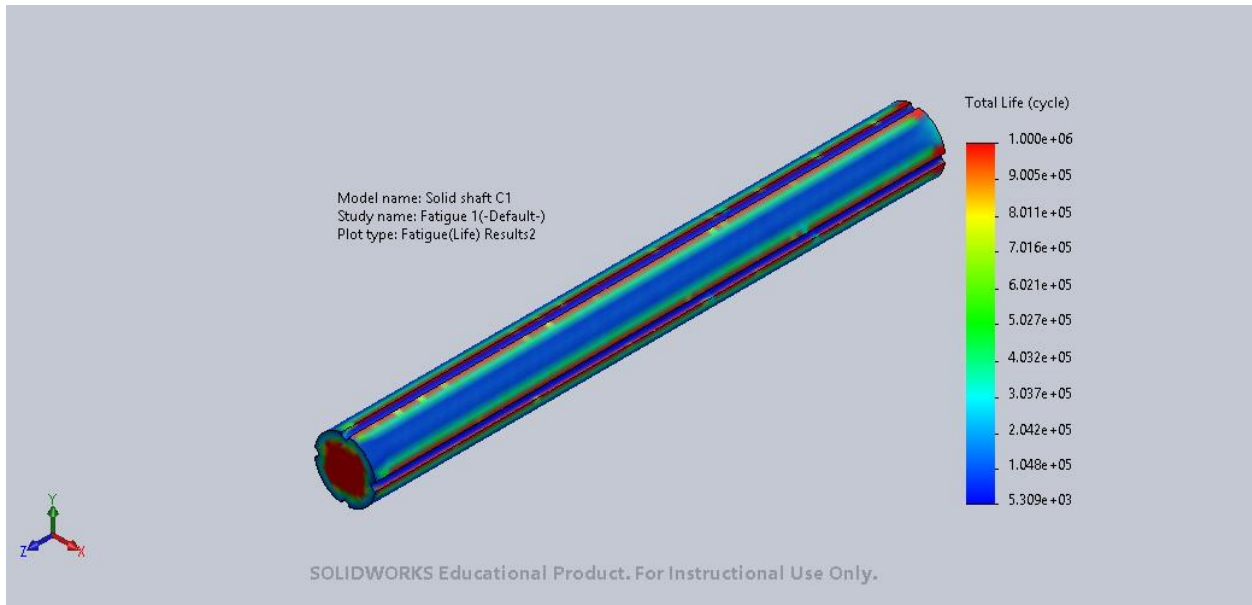
Figure 13
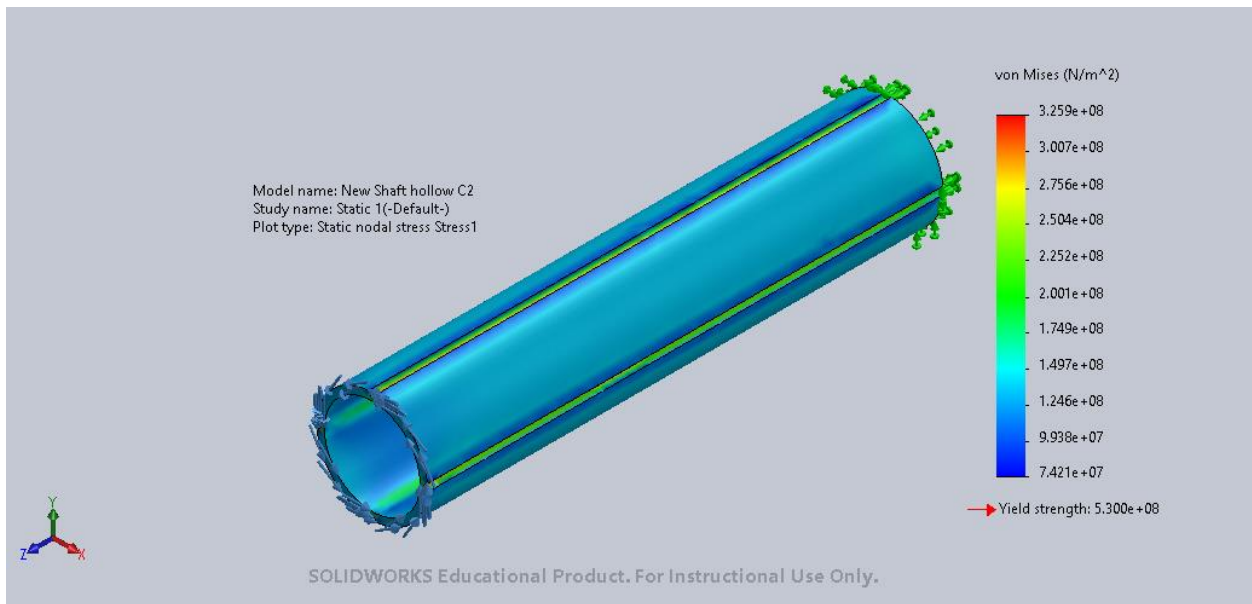
Figure 14
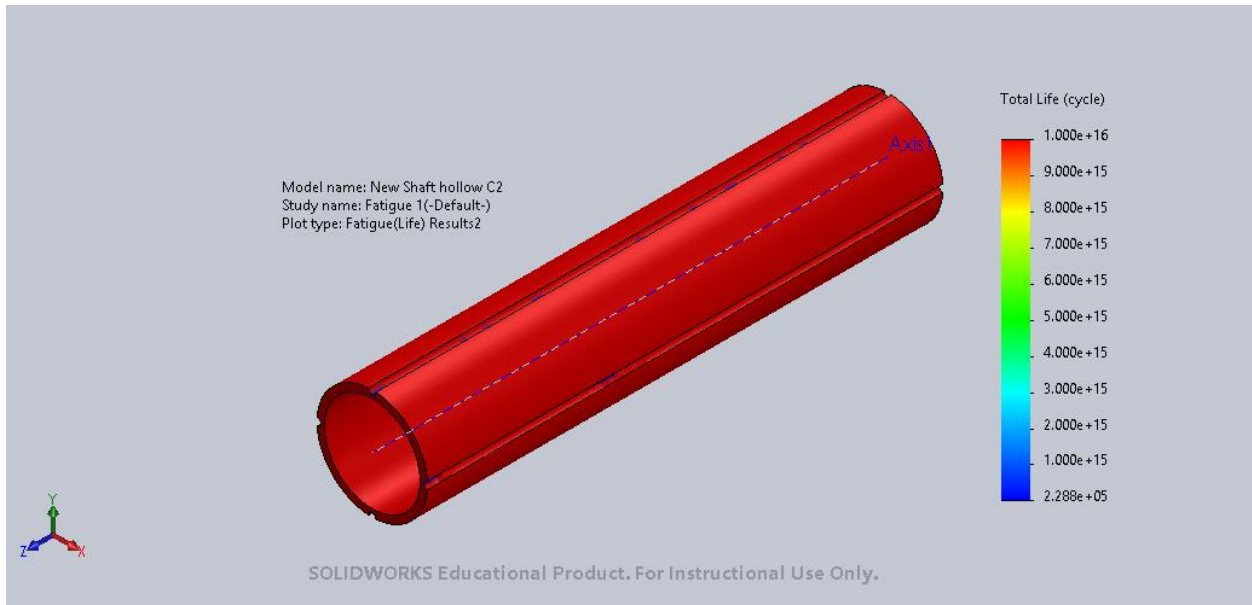
Figure 15
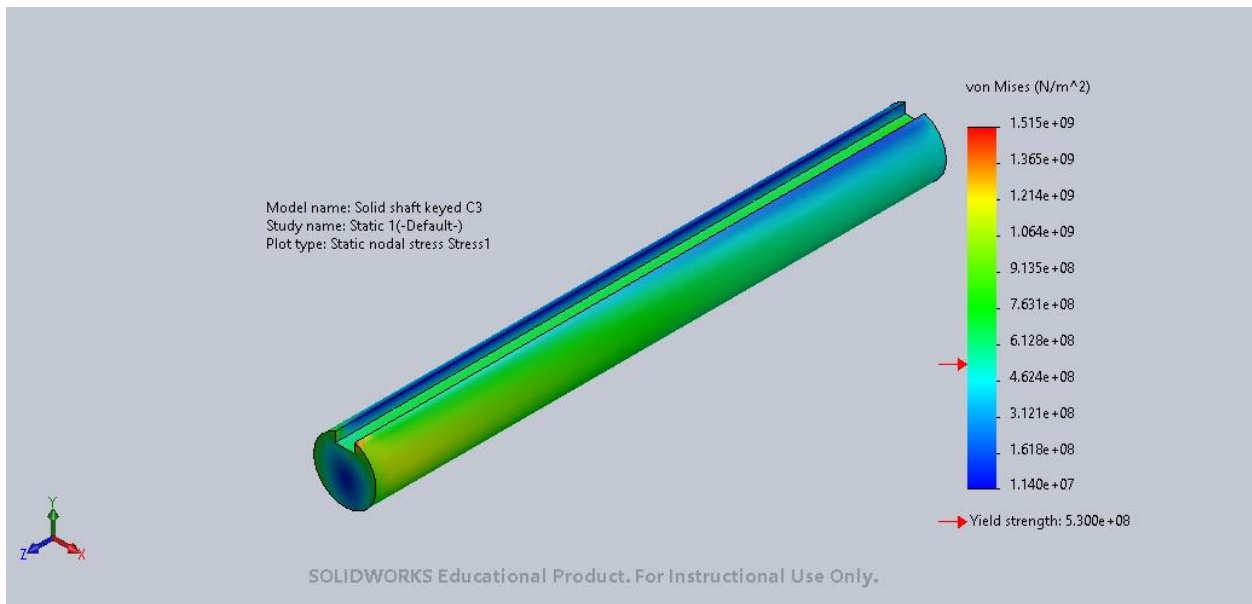
Figure 16
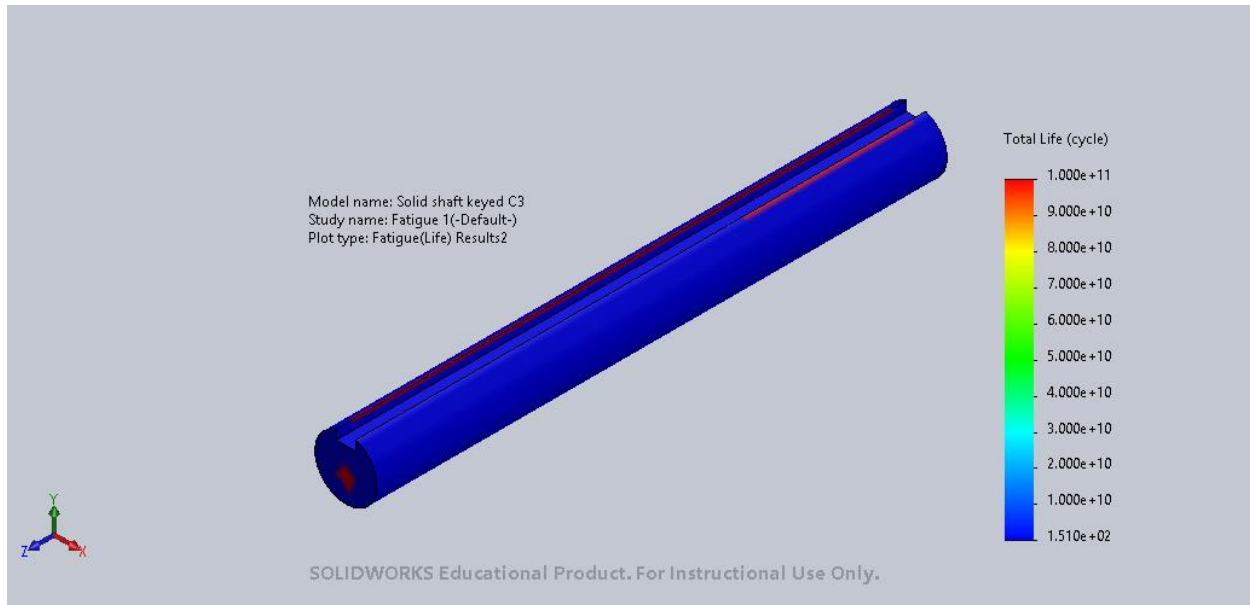
Figure 17

Additionally, the belt did not exhibit any slippage at the over-driven 57.9Nm of torque. This finding should be compared to the estimated maximum of 180Nm that a professional cyclist would be able to exert on the same pulley.

Discussion

In general, we can see that the efficiencies that were shown through the efficiency testing were not exactly on par with efficiencies expected from traditional/ conventional derailleur drivetrains. The prototype tested was able to experience efficiency up to 94%, where conventional derailer based drivetrains can achieve efficiencies up to 97% (Denham, 2017).

However, the efficiency testing produced was able to produce results that show a fairly defined trend that indicates that the efficiency can be further improved. In Figures 6 and 7 it can be seen that the maximum efficiency achieved occurs between the maximum and minimum tensions. As tension increases to its extreme (the tension ratio becomes smaller) in all cases the efficiency decreases to its smallest value. As the tension decreases to its extreme (the ratio becomes larger) in most cases the efficiency decreases from the measurement of its peak. This implies a moderate middle ground tension produces the highest efficiency and that different factors cause a drop off efficiency. Without further research, it is hard to determine exactly what caused the varying levels of efficiency, but the most likely cause of the drop in efficiency experienced with low tension is wasted energy due to the belt sliding relative to the pulley. When

the belt slips, some of the mechanical power that it is transferring is converted into energy in the form of heat, resulting in that energy not reaching the other side of the transmission, hence a lower efficiency. Likewise, when the tension is too great, a drop off of efficiency can most likely be explained by internal friction of the belt. More force is applied to the belt in the form of tension the more the internal of the belt are strained and basically rub against each other. This internal turmoil creates heat at the molecular level, causing the problem of lost energy in the form of heat as described above. Establishing an ideal tension is helpful when determining how to set the tension of the belt if the tension is being set using the preload. The preload would need to be enough to push the belt out relative to the shaft so that the desired level of tension is experienced but not too much as to exceed it.

Additionally, it can be seen that the cross-sectional area of the belt made a significant difference where the wider belt with a larger cross-sectional area was less efficient than the narrower belt with a relatively smaller cross-sectional area. This tells us there is hope at improving the efficiency of this transmission by changing the characteristics such as the cross-sectional area of the belt.

According to Figures 11 and 12 we can see that there was not a noticeable difference between the different radius configurations between the belts for almost all configurations, the only sizable exception being the smallest radius configuration on the narrow belt. Establishing a minimum radius threshold for a belt would be very beneficial to development since it would establish a max and min range for the effective belt radius for a given belt (max determined by the circumference since the pulleys have to be in line) helping either fix a belt selection for a target gear ratio range, or fix a gear ratio range for a given belt (say the belt with the smallest cross sectional area that is readily available from major suppliers). One possible explanation for this decrease in efficiency once the radius gets too small can be found in the cogged nature of the belts being tested. The belts have a cogged design that enables them to retain a smaller cross sectional as they bend around the pulleys while retaining a larger contact patch area than that which would be achieved if the whole belt had a smaller cross-sectional area/ depth. If the radius gets too small, the cogs could possibly start to touch each other as they travel around the pulley, effectively greatly increasing the cross-sectional area of the belt.

The slippage of the belt throughout the testing appeared to be satisfactory, however, it is important to note that 57.9Nm is only about a third of the estimated maximum torque that a professional cyclist would be able to apply to a shaft, indicating that this metric is not too reliable for determining the overall tendency to slip of the belt. Also, since tension on the belt affects the friction force between the belt and the pulley, it is important to note that spillage could be stopped by increasing the tension, however this might impact efficiency.

Analyzing the life duration results for the actuation device and the attachment of the actuation device to the pulley half, it is possible to see that there is great potential to improve the life of the part. By increasing the number of holes, it is possible to better distribute the load into the areas where there is a very high life (indicated by the red on figure 13). The European Committee for Standardization recommends a life span of 100,000 cycles for bicycle crank arms

(Gutiérrez-Moizant, R., Ramírez-Berasategui, M., Calvo, J. A., & Álvarez-Caldas, C., 2020), thus it is reasonable to assume that the life of a shaft connecting the crank arms and the pulley connected to the shaft should be able to withstand 200,000 cycles since there are two loading cycles on each shaft per full pedal rotation. When analyzing the life data found with different geometries and a similar arbitrary mass, it can be seen that the only shaft design that outperforms the rest is the hollow splined design. While the life of the solid splined design is only around 5,000 cycles, by changing the geometry to maximize a cavity, the life increases to over 200,000 cycles. The non-uniform nature of the keyed shaft caused it to perform the worst. While having around the same diameter as the solid splined shaft

There are many avenues for further study related to this project, the first of which involves fixing the actuation method of the transmission so that the ability to change mechanical advantage while mechanical power is being transmitted through the drivetrain. This could be accomplished using linear bearings to decrease/ effectively eliminate the friction between the bore of the pulley and the shaft (eliminating the reason that further testing of the proposed actuation method was not tested) The actuation method would need to be able to be small enough to fit inside a small area as to be able to fit between the pedals of a cyclist. Further, once the actuation method has been discovered, electronic capabilities can be developed to adjust mechanical advantage automatically as rider effort changes if a mechanical automatic means of adjustment is not possible. Self-actuation of the driven/ reaction pulley should also be tested. This would enable the actuation method to only affect one side of the transmission, greatly reducing the complexity. Other areas of further study include testing to see if sheaves using the Onyx (composite nylon) material would be able to achieve the same efficiencies and non-slip abilities as the aluminum sheaves used in the test described above. The weight of the prototype can also be re-assessed by optimizing the geometries of the components, in similar ways to those found for the shaft designs shown above.

Conclusion

The belt based CVT has potential to be applied in low torque, low RPM applications. Given that observed efficiency is relatively close to that achieved by conventional drivetrains and that trends that could lead to further efficiency improvement were observed, with further development, the efficiency of a drivetrain with this transmission could be comparable to that of a conventional drivetrain. The friction proved to be adequate however needs further testing to verify that under maximum torque produced by cyclists the belt will not slip. The strength of the first prototype proved to be adequate with no parts malfunctioning, and there appears to be many ways to further optimize strength to cut down on weight in later designs. Thus, the belt based CVT should be further developed for bicycles and definitely has potential.

References

Amilan™ Nylon Resin. TORAY. (n.d.). Retrieved October 5, 2021, from
    https://www.toray.jp/plastics/en/amilan/technical/tec_006.html.

Bhaumik, S. K., Sujata, M., & Venkataswamy, M. A. (2007, October 12). *Fatigue failure of
    aircraft components*. Engineering Failure Analysis. Retrieved October 5, 2021, from
    https://www.sciencedirect.com/science/article/pii/S1350630707001409.

Boyer, H. E. (2010). *Atlas of Fatigue Curves*. ASM International.

Chamberlin, D. (2017, October 4). *What is a CVT transmission?* What is a CVT Transmission? |
    Car Reviews Canada | New & Used Automotive News and Tips | | Go Auto. Retrieved
    October 5, 2021, from https://www.goauto.ca/blog/what-is-a-cvt-transmission.

David Rouffet PhD. (2021, August 18). *Track Cycling World Championships – the making of
    modern sprinters*. The Conversation. Retrieved October 5, 2021, from
    https://theconversation.com/track-cycling-world-championships-the-making-of-modern-
    sprinters-6235.

Demhan. (2017, August 2). *What's the difference in speed between gearbox systems? Rohloff,
    pinion, shimano*. CyclingAbout. Retrieved October 5, 2021, from
    https://www.cyclingabout.com/speed-difference-testing-gearbox-systems/.

Denham. (2019, April 3). *11 reasons to tour with a pinion gearbox ... - cyclingabout*. Retrieved
    October 5, 2021, from https://www.cyclingabout.com/tour-with-a-pinion-gearbox/.

eFunda, I. (n.d.). *Home*. The S-N Curve. Retrieved October 5, 2021, from
    https://www.efunda.com/formulae/solid_mechanics/fatigue/fatigue_highcycle.cfm.

Fan application - greenheck-USA. (n.d.). Retrieved October 5, 2021, from
    https://content.greenheck.com/public/DAMProd/Original/10002/FA127-11.pdf.

Gutiérrez-Moizant, R., Ramírez-Berasategui, M., Calvo, J. A., & Álvarez-Caldas, C. (2020,
    March 25). *Validation and improvement of a bicycle crank arm based in numerical
    simulation and uncertainty quantification*. Sensors (Basel, Switzerland). Retrieved October
    5, 2021, from https://www.ncbi.nlm.nih.gov/pmc/articles/PMC7180959/.

Onyx - composite 3D printing material. Markforged. (n.d.). Retrieved October 5, 2021, from
    https://markforged.com/materials/plastics/onyx.

Ozdemir, O., Bala, Nick, Inventions, O., Deey, H., Banerjee, deboprasad, Nair, S., Pushati, K.,
    Yahya, Essien, Srinivas, Deepak, Simplemotor, Xu, C., Khan, M. R., Chaudhary, M.,
    Alferez, ojong, L. ayuk, Dayi, T., … Kalulu, G. (2014, March 13). *Calculations*. Simple
    Electric Motors. Retrieved October 5, 2021, from https://simplemotor.com/calculations/.

Rudd, J., Hahin, C., & Banas, G. (2013). *Fatigue performance of brass breakaway light pole couplings*. Illinois Center for Transportation.

Stebbins, C. L., Moore, J. L., & Casazza, G. A. (2014, January 20). *Effects of cadence on aerobic capacity following a prolonged, varied intensity cycling trial*. Journal of sports science & medicine. Retrieved October 5, 2021, from https://www.ncbi.nlm.nih.gov/pmc/articles/PMC3918546/.

Works cited (number of source in parenthesis in draft report where info pops up)

1. https://www.sciencedirect.com/science/article/pii/S1350630707001409 article about what fatigue is
2. https://www.efunda.com/formulae/solid_mechanics/fatigue/fatigue_highcycle.cfm for S-N curve for 1045 steel
3. https://core.ac.uk/download/pdf/16504225.pdf S-N curve for 360 Brass (61%cu 36.6% Zn)
4. https://kupdf.net/download/atlas-of-fatigue-curves_58bd7994e12e89fb3fadd378_pdf S-N curve for 304 stainless
5. https://www.toray.jp/plastics/en/amilan/technical/tec_006.html S-N curve for nylon 6
6. https://simplemotor.com/calculations/ the motor torque equation while rotating
7. https://theconversation.com/track-cycling-world-championships-the-making-of-modern-sprinters-6235 max watts and estimated rpm expended by male etc.
8. https://content.greenheck.com/public/DAMProd/Original/10002/FA127-11.pdf Belt tension calculation. Might need to do a ratio of tensions etc. since i have bad units etc
9. https://www.ncbi.nlm.nih.gov/pmc/articles/PMC3918546/ The optimal pedal cadance and its effect of rider maximal effort expendeture.
10. https://markforged.com/materials/plastics/onyx nylon Filament
11. Denham, A. (2017, August 2). What's the difference in speed Between GEARBOX Systems? Rohloff,Pinion, Shimano. Retrieved March 11, 2021, from https://www.cyclingabout.com/speed-difference-testing-gearbox-systems/
12. Denham, A. (2019, April 3). 11 reasons to tour with a PINION GEARBOX (and 8 reasons to not).Retrieved March 11, 2021, from https://www.cyclingabout.com/tour-with-a-pinion-gearbox/
13. Gutiérrez-Moizant, R., Ramírez-Berasategui, M., Calvo, J. A., & Álvarez-Caldas, C. (2020, March 25). *Validation and improvement of a bicycle crank arm based in numerical simulation and uncertainty quantification*. Sensors (Basel, Switzerland). Retrieved September 23, 2021, from https://www.ncbi.nlm.nih.gov/pmc/articles/PMC7180959/.
14. https://www.goauto.ca/blog/what-is-a-cvt-transmission pictue of cvt